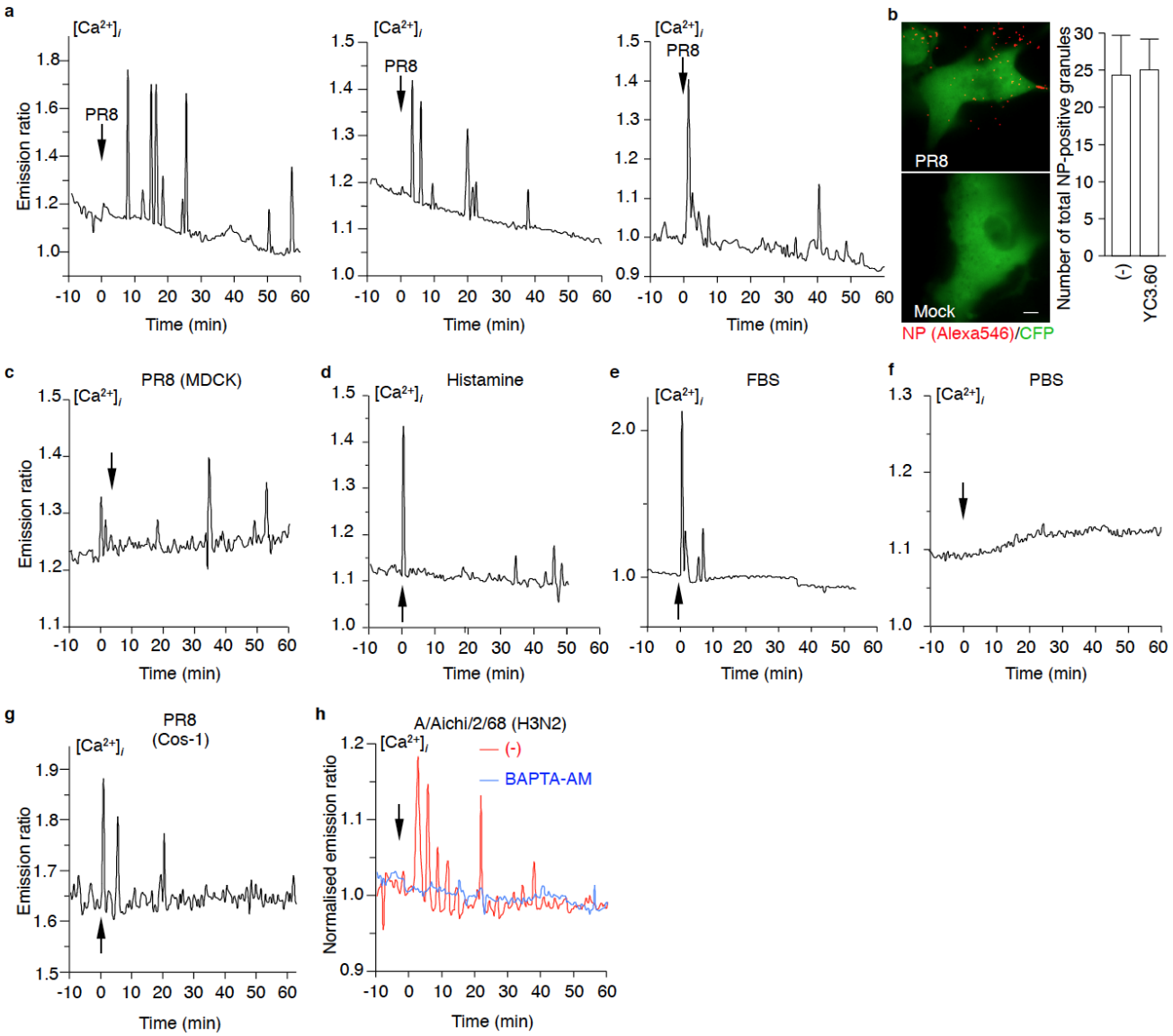
HOKKAIDO UNIVERSITY

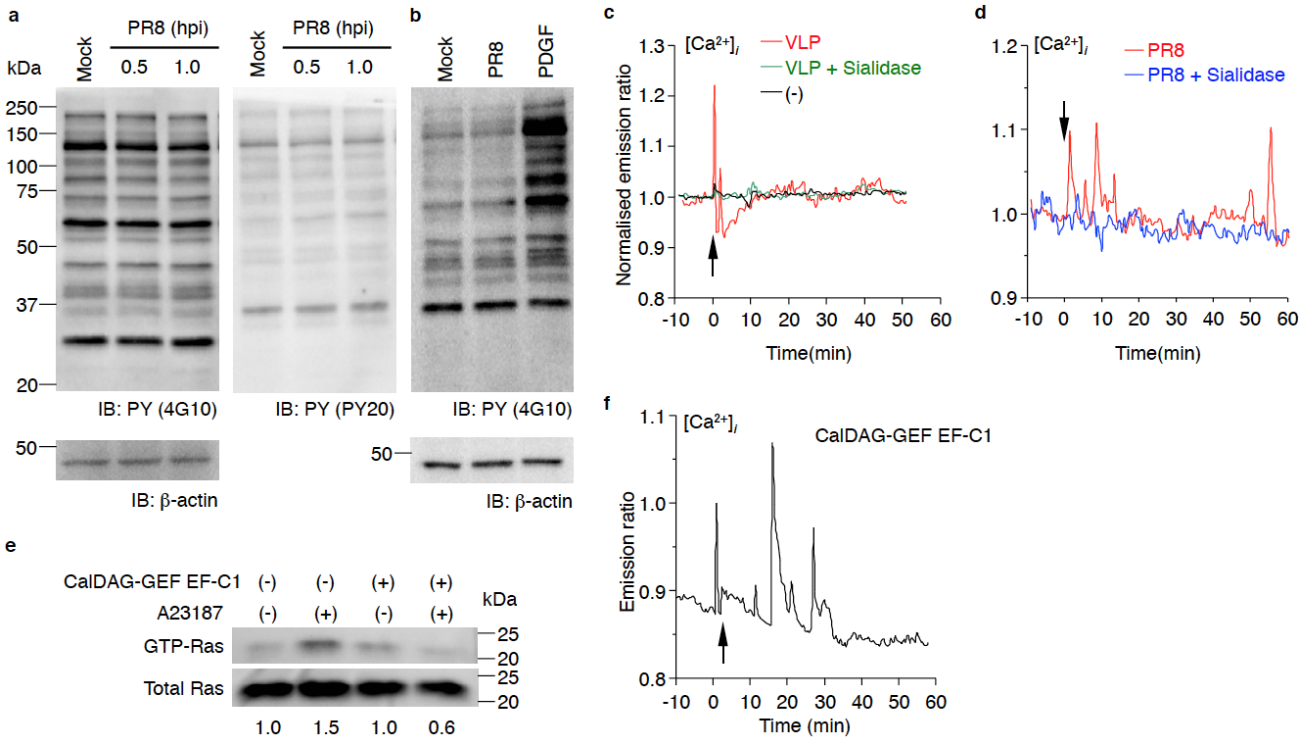
Title	A Ca2+-dependent signalling circuit regulates influenza A virus internalization and infection
Author(s)	Fujioka, Yoichiro; Tsuda, Masumi; Nanbo, Asuka et al.
Citation	Nature communications, 4, 2763 https://doi.org/10.1038/ncomms3763
Issue Date	2013-11-14
Doc URL	https://hdl.handle.net/2115/55820
Type	journal article
File Information	supplementary information.pdf

Hokkaido University Collection of Scholarly and Academic Papers : HUSCAP

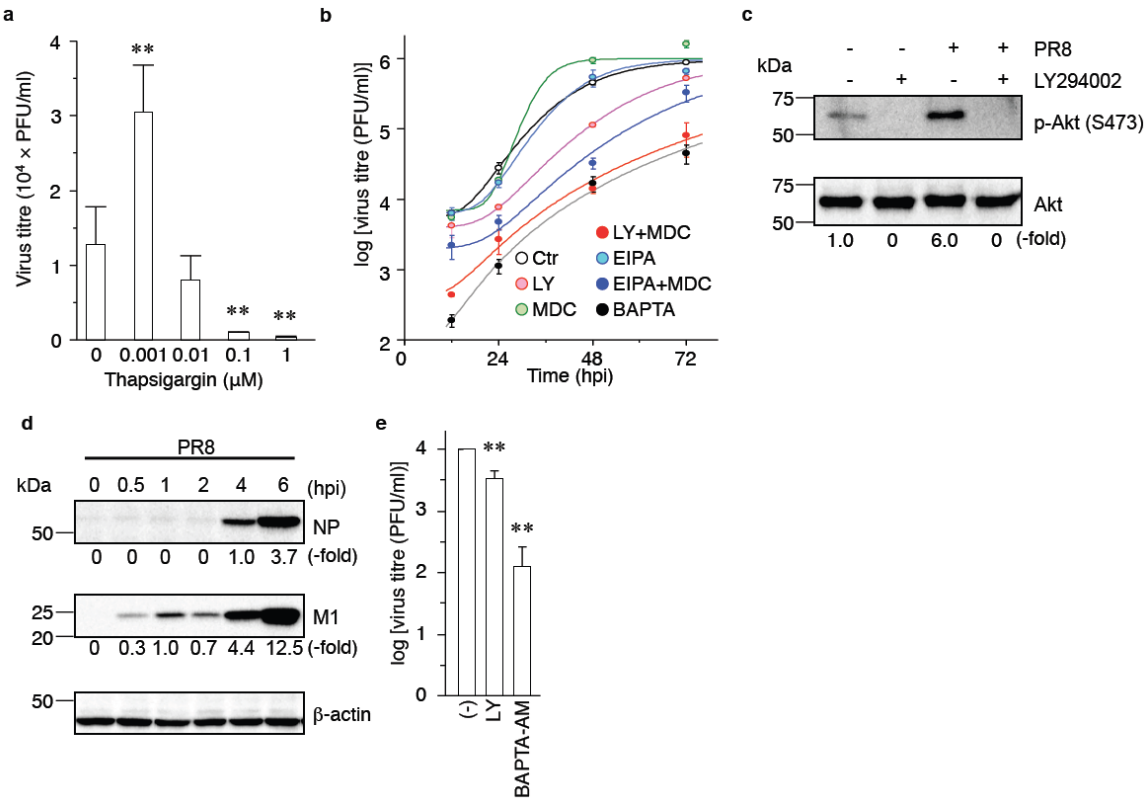
Supplementary Figures S1–S15



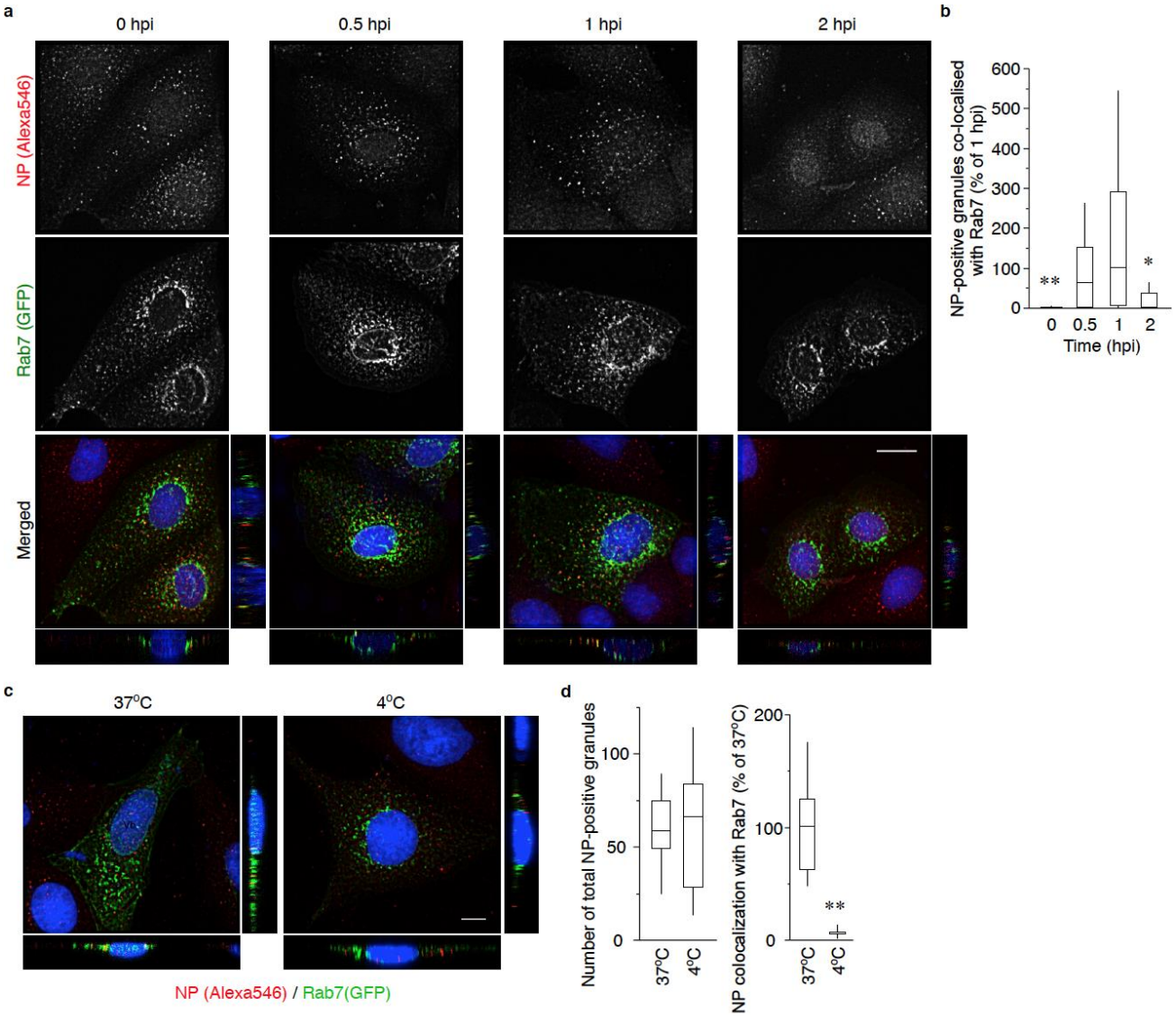
Supplementary Figure S1 | Ras activation by IAVs is mediated by intracellular Ca^{2+}. (**a**) Three representative examples of $[Ca^{2+}]_i$ oscillations evoked by infection of MEFs with PR8 at time 0 (left three panels). (**b**) The cells shown in Fig. 1a were fixed following to time-lapse observation and subjected to immunofluorescence to confirm that the cells were indeed exposed to IAV particles. Bar, 10 μm. Numbers of NP-positive granules in cells in the presence or absence of expression of YC3.60 were also counted and plotted (right panel). Error bars indicate s.d. (*n* =10) (**c**–**f**) MDCK cells expressing YC3.60 were infected with PR8 (**c**), stimulated with 100 μM histamine (**d**) or 10% (final concentration) FBS (**e**) at time 0. PBS (5 μl) was used as a negative control (**f**). The $[Ca^{2+}]_i$ was monitored by FRET imaging. (**g**) Cos-1 cells expressing YC3.60 were infected with PR8 at time 0. The $[Ca^{2+}]_i$ was monitored as described above. (**h**) Cos-1 cells expressing YC3.60 were incubated in the absence or presence of 25 μM BAPTA-AM for 30 min before infection with A/Aichi/2/68 (H3N2) at time 0. The $[Ca^{2+}]_i$ was monitored by FRET imaging.



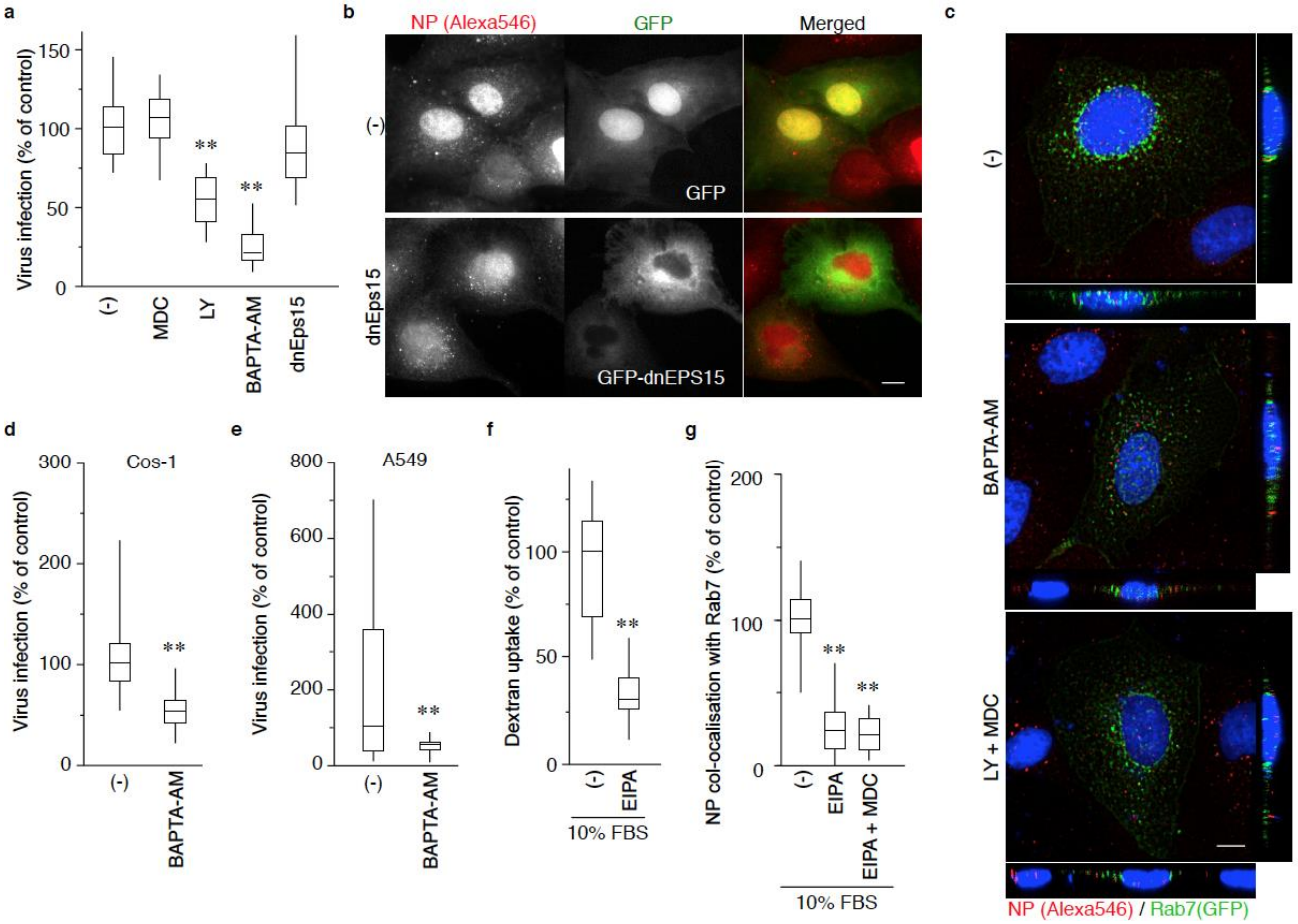
Supplementary Figure S2 | Ras activation by IAVs is mediated by intracellular Ca^{2+}. (**a**) MEFs either infected with PR8 for 0.5 or 1 h, or subjected to mock infection, were lysed and subjected to immunoblot analysis (IB) with antibodies to phosphotyrosine (clones 4G10 or PY20) or to β-actin (loading control). (**b**) MEFs either infected with PR8 for 30 min, stimulated with PDGF at 50 ng/ml for 10 min, or left untreated (Mock) were analysed by IB with the 4G10 antibodies. (**c**) 293T cells were transfected with expression vectors for PR8 HA, NA, M1 and M2 (VLP) or control vectors (-), and the culture supernatants were collected at 48 h after transfection. Cos-1 cells expressing YC3.60 were incubated in the absence or presence of 5 mU/ml sialidase for 30 min before exposure to the culture supernatants at time 0 and were monitored by dual-emission fluorescence microscopy. Normalised emission ratio against time was plotted. (**d**) Cos-1 cells expressing YC3.60 were incubated in the absence or presence of 5 mU/ml sialidase for 30 min before exposure to PR8 at time 0 and were monitored by dual-emission fluorescence microscopy. Normalised emission ratio against time was plotted. (**e**) Cos-1 cells were transfected with expression vectors for the EF-C1 domain of CalDAG-GEFII or control vectors and after 24 h, stimulated by the calcium ionophore A23187 for 30 min. Ras activity was determined by the Bos pulldown method. (**f**) Cos-1 cells expressing YC3.60 alone or together with the EF-C1 domain of CalDAG-GEFII were infected with PR8 at time 0 and monitored by dual-emission fluorescence microscopy.



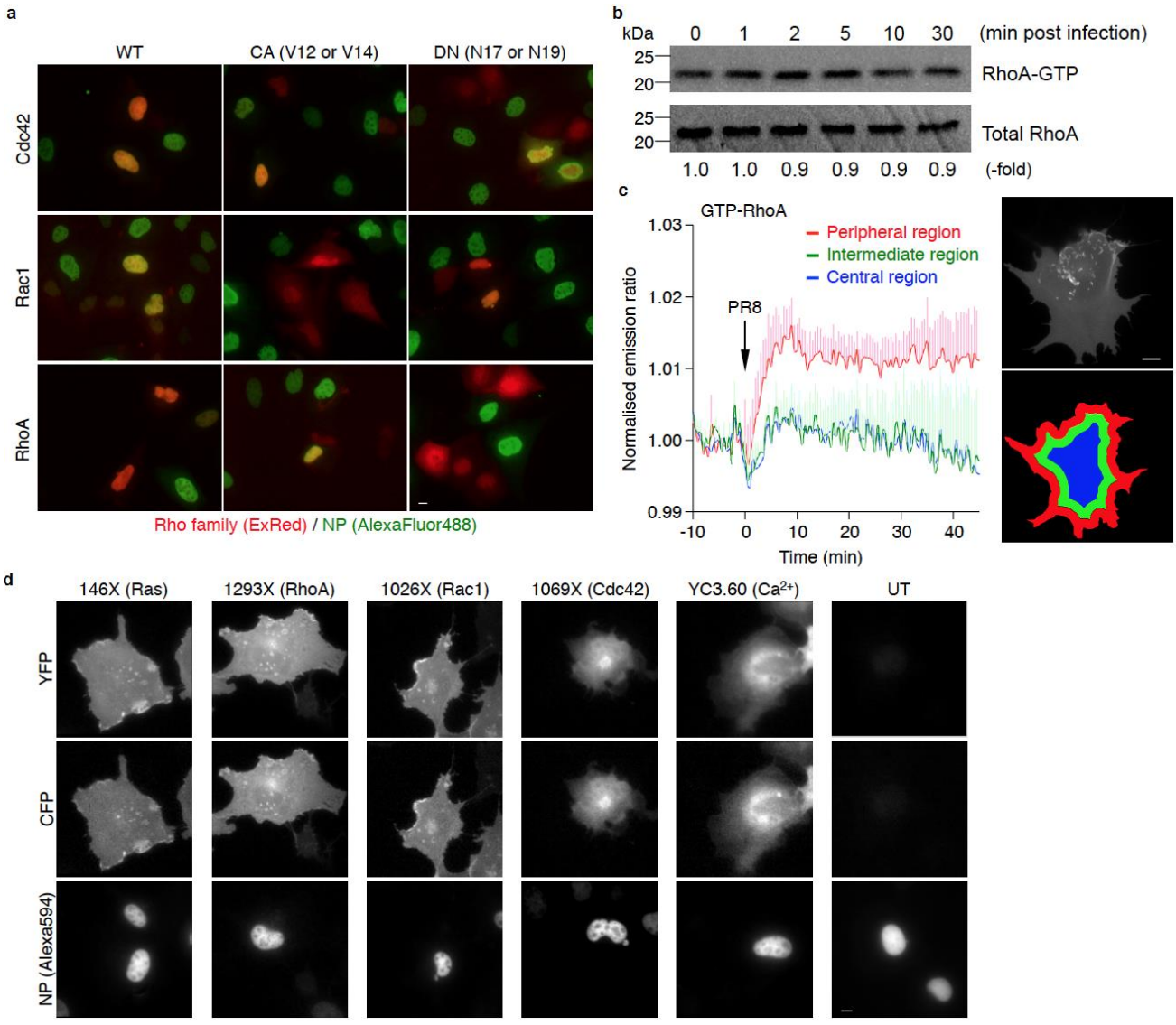
Supplementary Figure S3 | Calcium signalling is a key regulator of IAV infection. (**a**) MDCK cells were incubated in the presence of thapsigargin at indicated concentrations for 30 min before infection with PR8 at an MOI of 1 PFU/cell for 1 h. The titre of infectious virus particles released into culture supernatants during the continued presence of test agents was determined with an MDCK plaque assay at 48 hpi. Data are means ± SD of values obtained from three independent experiments (n = 3 each). **P < 0.01 versus no treatment (0 μM) (Student's t-test). (**b**) MDCK cells were incubated in the absence (-) or presence of inhibitors, as indicated, for 30 min before infection with PR8 at an MOI of 1 for 1 h. The titre of infectious virus particles released into culture supernatants during the continued presence of test agents was determined with an MDCK plaque assay at indicated time points. Data are means ± SD obteained from three independent experiments (n = 3 each). (**c**) MDCK cells were incubated in the absence or presence of 50 μM LY294002 for 30 min, and were then infected with PR8 at an MOI of 1 for 4 h or left uninfected. The cells were lysed and subjected to immunoblot analysis with antibodies to phospho-Akt (S473) or Akt (loading control). (**d**) MDCK cells, infected with PR8 for indicated periods, were lysed and subjected to immunoblot analysis with antibodies to NP, M1 or β-actin (loading control). (**e**) MDCK cells were incubated in the absence or presence of 50 μM LY294002 or 25 μM BAPTA-AM for 30 min before, during and for 4 h after, infection with PR8 for 1 h. The titre of infectious virus particles released into culture supernatants was determined with an MDCK plaque assay at 48 hpi. Data are means ± SD from three independent experiments (n = 3 each). **P < 0.01 versus no treatment (–) (Student's t-test).



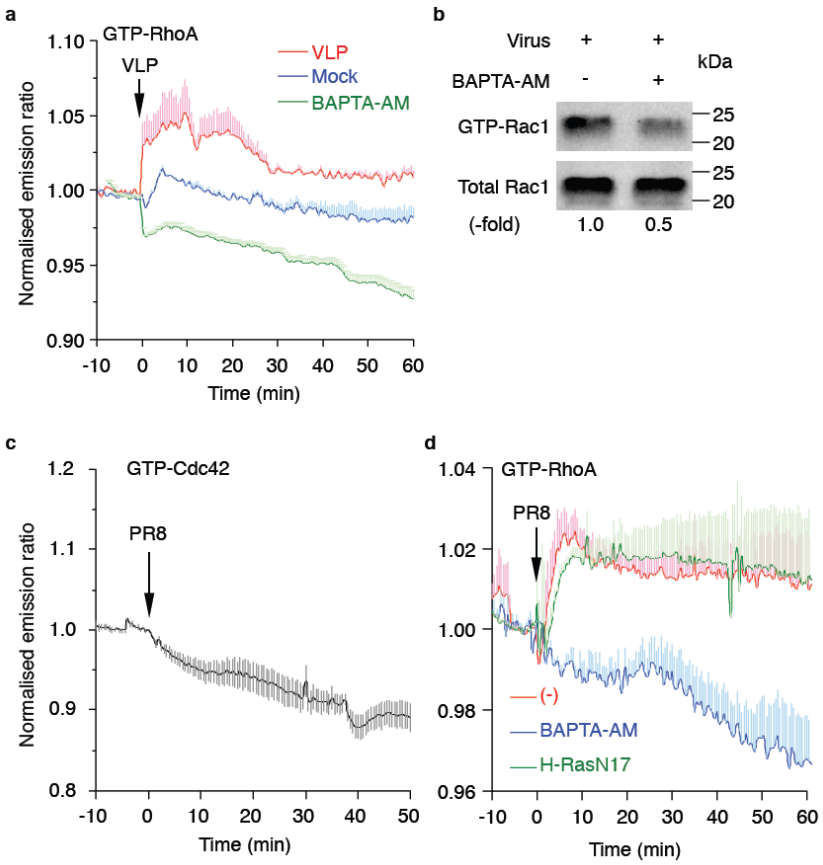
Supplementary Figure S4 | Calcium signalling is a key regulator of IAV infection. (**a**, **b**) MDCK cells transfected with an expression vector encoding GFP-Rab7 for 24 h were infected with PR8. The cells were then fixed at each time point (as indicated) and subjected to immunofluorescence staining with antibodies to NP. Nuclei were visualised by Hoechst 33342. A series of sections, covering from the top to the bottom of cells, was obtained with the use of a confocal microscope and was projected onto a single image plane to simultaneously visualize all virus particles and Rab7-positive granules therein. Representative projection images are shown for each indicated time point (**a**). Black and white images for each colour channel are also shown. Bar, 10 μm (**a**). Rab7- and NP-positive granules were extracted and their co-localisation was determined with the use of image processing software (**b**). *$P < 0.05$, **$P < 0.01$ versus 1 hpi (Student's *t*-test, $n = 10$). (**c**, **d**) MDCK cells expressing GFP-Rab7 were infected with PR8 for 1 h at either 37°C or 4°C. Representative projection images along with tangential (*xz* and *yz*) images, obtained as in (**a**), are shown (**c**). Bar, 10 μm. The number of total NP-positive granules and co-localisation of NP and GFP-Rab7 were quantitated and plotted (**d**). **$P < 0.01$ versus 37°C (Student's *t*-test, $n = 10$). The highest and lowest boundaries of the box represent the 25th and 75th percentiles, the whiskers above and below the box designate the 5th and 95th percentiles and the line within the box indicates the median value (b, d).



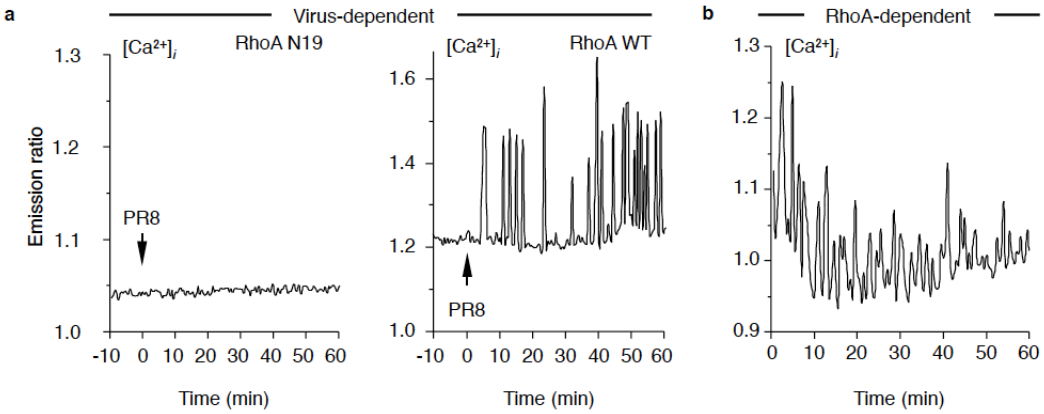
Supplementary Figure S5 | Calcium signalling is a key regulator of IAV infection. (**a**, **b**) MDCK cells transfected with an expression vector encoding GFP were incubated in the absence or presence of 25 μM BAPTA-AM, 50 μM LY294002 (LY) or 50 μM MDC for 30 min, and then incubated with PR8 for 4 h. MDCK cells expressing the dominant-negative form of Eps15 (dnEps15) tagged with GFP were also infected with PR8. The cells were then fixed and subjected to immunofluorescence staining with antibodies to the virus protein NP. Virus infection was determined on the basis of fluorescence intensity and plotted (**a**). $^{**}P < 0.01$ versus no treatment (–) (Student's *t*-test, $n = 20$). Representative images for control cells and GFP-dnEps15-transfected cells are also shown (**b**). Bar, 10 μm. (**c**) MDCK cells transfected with an expression vector for GFP-Rab7 were incubated in the absence or presence of BAPTA-AM or LY and MDC (LY + MDC) for 30 min before infection with PR8 for 1 h at 37°C. DMSO was used as a negative control. The cells were then fixed and subjected to a virus internalisation assay, as in (Supplementary Figure S4a). In addition to *xy*-projection images, tangential (*xz* and *yz*) images are also shown. Bar, 10 μm. (**d**, **e**) Cos-1 (**d**) or A549 (**e**) cells were incubated in the absence or presence of BAPTA-AM for 30 min before infection with PR8 for 4 h. The proportion of cells containing virus was determined by immunofluorescence staining with antibodies to NP and is expressed as a percentage of the corresponding value for control cells. Data are from three independent experiments. $^{**}P < 0.01$ versus no treatment (–) (Student's *t*-test, $n = 20$). (**f**) MDCK cells were incubated in the absence or presence of EIPA for 30 min before exposure to fluorescently labelled dextran for 10 min in the presence of 10% FBS. $^{**}P < 0.01$ versus no treatment (–) (Student's *t*-test, $n = 20$) (**g**) MDCK cells expressing GFP-tagged Rab7 were exposed to EIPA or EIPA along with MDC for 30 min and infected with PR8 for 1 h in the presence of 10% FBS. The cells were then fixed, subjected to immunofluorescence staining with antibodies to the virus protein NP and imaged with a confocal microscope. The number of virus particles co-localising with Rab7-positive vesicles was quantified and plotted. $^{**}P < 0.01$ versus no treatment (–) (Student's *t*-test, $n = 20$). The boundaries of the box, the whiskers above and below the box and the line within the box represent the 25th and 75th percentiles, the 5th and 95th percentiles and the median value, respectively (a, d–g).



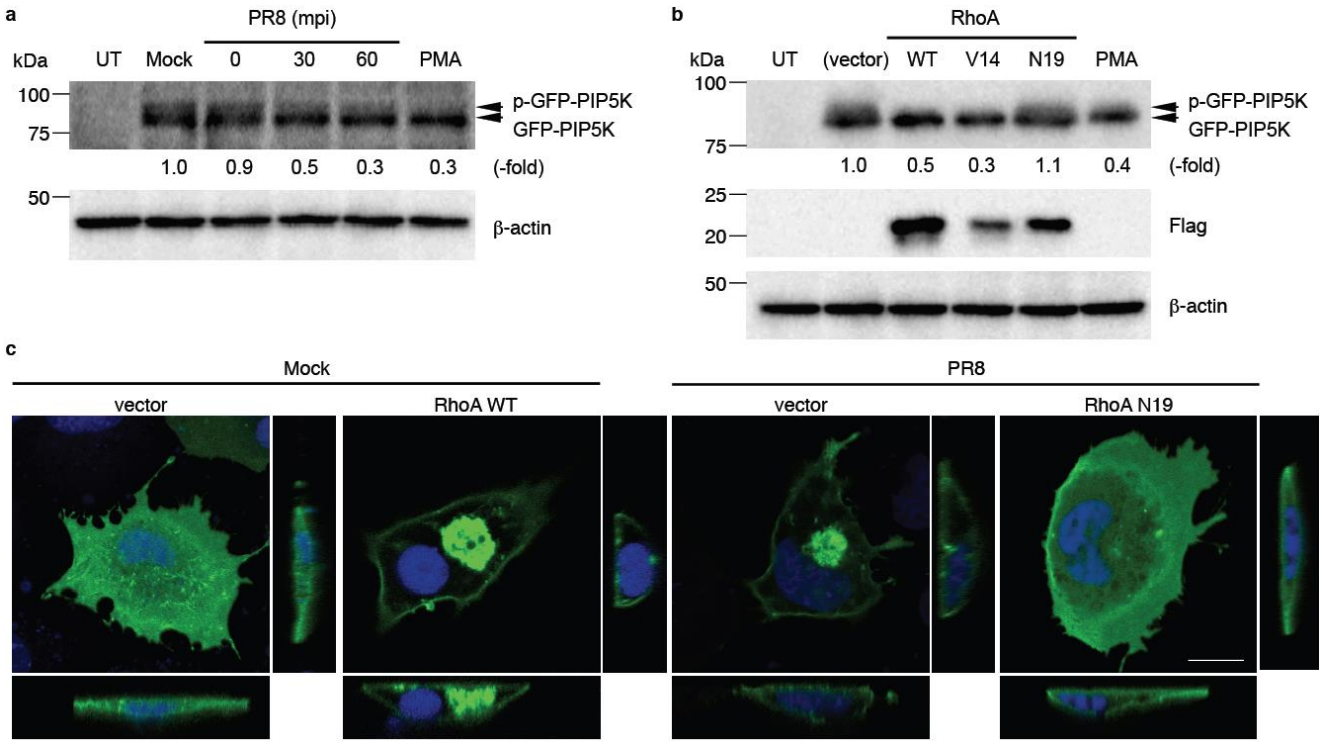
Supplementary Figure S6 | IAV internalisation is regulated by Rho family GTPases. (**a**) MDCK cells were transfected with expression vectors for wild-type (WT), constitutively active (CA) or dominant negative (DN) forms of Rho family GTPases for 24 h, incubated with PR8 for 4 h, then fixed and subjected to immunofluorescence staining with antibodies to NP for detection of replicated viruses. Expression of GTPases was indicated by the fluorescence of ExRed encoded by the bicistronic vectors. Bar, 10 μm. (**b**) Cos-1 cells infected with PR8 for indicated periods were lysed and subjected to a pull-down assay followed by immunoblot analysis to determine the activity of endogenous RhoA. The intensity of the bands was quantitated by an image analyser and the fold increase in GTP-bound/total RhoA is shown at the bottom. (**c**) Cos-1 cells expressing Raichu-RhoA were monitored by dual-emission fluorescence microscopy with exposure to PR8 at time 0. The cell area was divided into three regions (peripheral [red], intermediate [green], central [blue]), and RhoA activity (FRET/CFP ratio) in each region was plotted over time. Error bars indicate s.e.m. (n = 12) (**d**) Cos-1 cells expressing Raichu-146X, 1293X, 1026X, 1069X or YC3.60 were infected with PR8 for 4 h, then fixed and subjected to immunofluorescence staining with antibodies to NP. UT, untransfected. Bar, 10 μm.



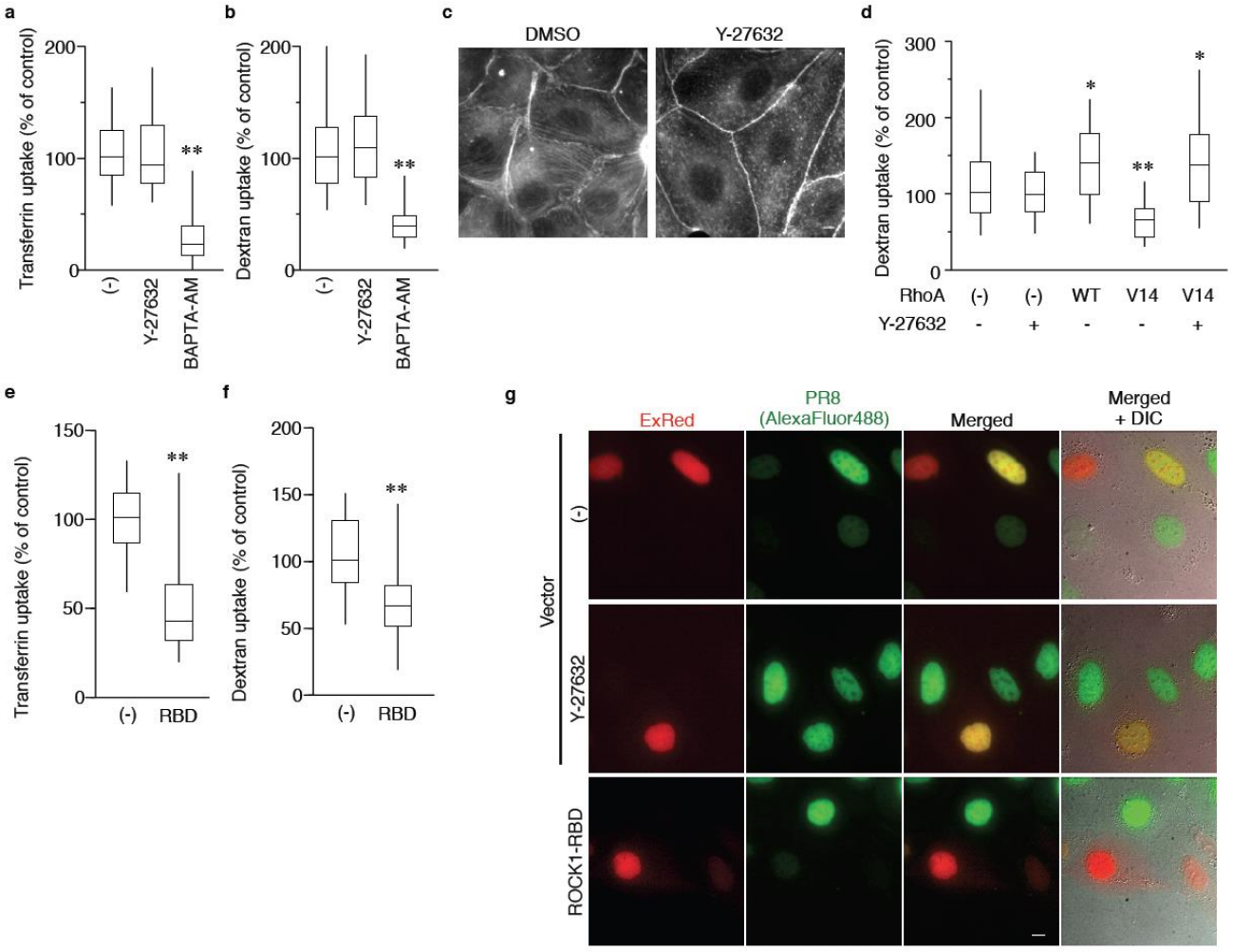
Supplementary Figure S7 | IAV internalisation is regulated by Rho family GTPases. (**a**) Cos-1 cells expressing Raichu-RhoA, with or without pre-treatment with BAPTA-AM, were monitored by dual-emission fluorescence microscopy with exposure to culture media containing VLPs or those from mock transfected cells, as indicated. RhoA activity (normalised FRET/CFP emission ratio) at the peripheral region of the cells was plotted, as in (Supplementary Figure 6c). Error bars indicate s.e.m. (n = 4) (**b**) Cos-1 cells were incubated in the absence or presence of 25 μM BAPTA-AM for 30 min before infection with PR8 for 5 min. Cell lysates were then prepared and subjected to a pull-down assay followed by immunoblot analysis to determine the activity of Rac1. (**c**) Cos-1 cells expressing Raichu-Cdc42 were infected with PR8 at time 0, and the activity of Cdc42 was monitored as the normalised FRET/CFP emission ratio. Error bars indicate s.e.m. (n = 6) (**d**) Cos-1 cells expressing Raichu-RhoA and the dominant negative mutant of Ras (Ras N17) were monitored by dual-emission fluorescence microscopy with exposure to PR8 at time 0 (green). Cos-1 cells expressing Raichu-RhoA were incubated in the absence (red) or presence of BAPTA-AM (blue) for 30 min before exposure to PR8 at time 0. RhoA activity at the peripheral region of the cells was plotted, as in (Supplementary Figure 6c). Error bars indicate s.e.m. (n = 6)



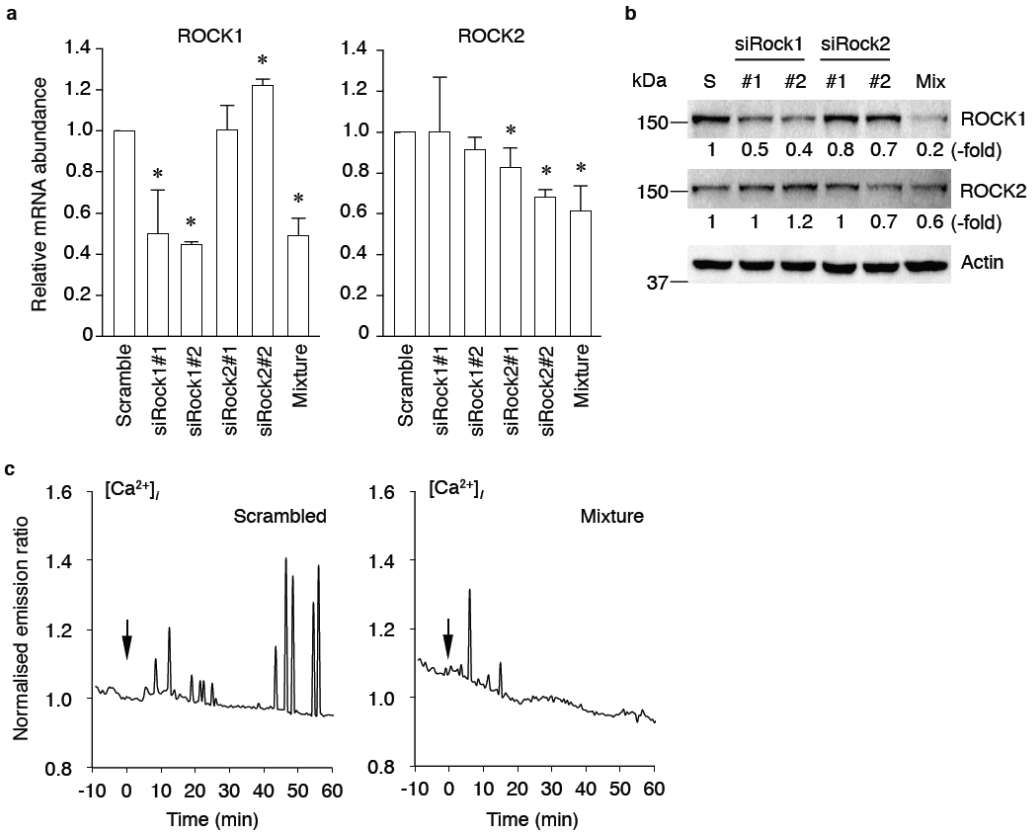
Supplementary Figure S8 | RhoA enhances virus-induced $[Ca^{2+}]_i$ oscillation in MDCK cells. (**a**) MDCK cells were transfected for 24 h with expression vectors for YC3.60 and either the wild type (WT) (right panel) or the dominant negative mutant (N19) (left) of RhoA as indicated, infected with PR8 (at time 0) and subjected to time-lapse fluorescence microscopy. (**b**) MDCK cells expressing YC3.60 and RhoA were observed by fluorescence microscopy to monitor $[Ca^{2+}]_i$.



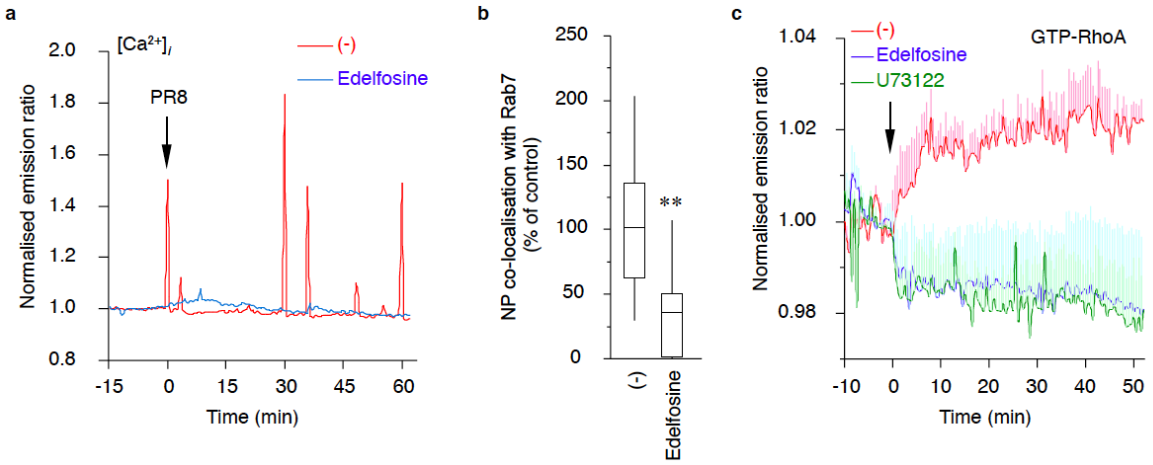
Supplementary Figure S9 | IAV infection activates PIP5K. (**a**) Cos-1 cells expressing GFP-PIP5K were infected with PR8 for indicated periods or were stimulated with PMA for 30 min. The cells were then lysed and subjected to immunoblot analysis. The relative phospho-PIP5K levels were determined and indicated at the bottom of the panel. UT, untransfected. (**b**) RhoA-dependent activation of PIP5K was analysed by immunoblotting as in (a). PMA stimulation (for 30 min) was also used as a positive control. vector, control vector-transfected cells. (**c**) Cos-1 cells expressing GFP-PIP5K alone (left panels) or together with dominant negative form of RhoA (RhoA N19, right lower panel) were infected with PR8 for 30 min (lower panels) or left uninfected (Mock, upper panels). Alternatively, cells expressing GFP-PIP5K and wild-type (WT) RhoA were also prepared (right upper panel). The cells were fixed with paraformaldehyde and observed with confocal microscopy. Nuclei were visualised by Hoechst 33342. Horizontal (*xy*) and tangential (*xz* and *yz*) images are shown. Bar, 10 μm.



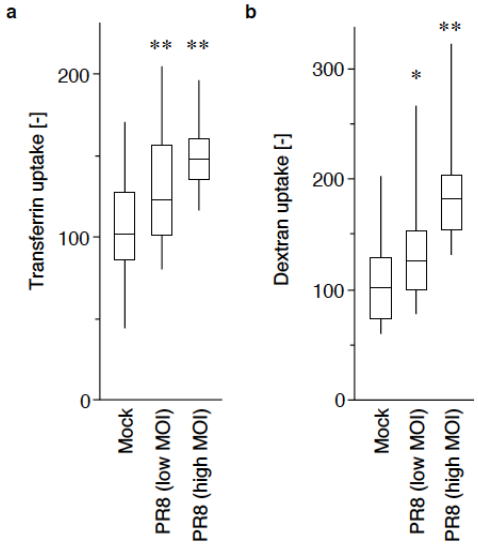
Supplementary Figure S10 | ROCK mediates RhoA signalling during IAV infection in a manner independent of its kinase activity. (**a**, **b**) MDCK cells were incubated in the absence or presence of Y-27632 or BAPTA-AM for 30 min before assay of endocytic activity with transferrin (**a**) or dextran (**b**). $^{**}P < 0.01$ versus control cells (Student's *t*-test, $n = 25$). (**c**) MDCK cells were incubated in the presence or absence of Y-27632, fixed and permeabilised. Actin stress fibres were visualised with the use of AlexaFluor 594-conjugated phalloidin. (**d**) Cos-1 cells transfected with expression vectors for wild-type (WT) or V14 mutant forms of RhoA or with a control vector were incubated for 16 h in the absence or presence of 10 μM Y-27632, as indicated, and were then assayed for dextran uptake. $^{*}P < 0.05$, $^{**}P < 0.01$ versus control cells (Student *t*-test, $n = 20$). (**e**, **f**) Cos-1 cells transfected with an expression plasmid for the RBD of ROCK1 or a control vector were assayed for endocytosis of transferrin (**e**) or dextran (**f**) $^{**}P < 0.01$ versus control cells (Student's *t*-test, $n = 20$). (**g**) Cos-1 cells were transfected for 24 h with an expression vector for the RBD of ROCK1 or a control vector and were then incubated for 30 min, in the absence or presence of Y-27632, as indicated, before infection with PR8 for 4 h. Replicated viruses were detected by immunofluorescence staining with antibodies to NP, and transfected cells were identified by the fluorescence of ExRed expressed from the bicistronic vector. DIC, differential interference contrast. Bar, 10 μm. The boundaries of the box, the whiskers above and below the box and the line within the box represent the 25th and 75th percentiles, the 5th and 95th percentiles and the median value, respectively (a, b, d–f).



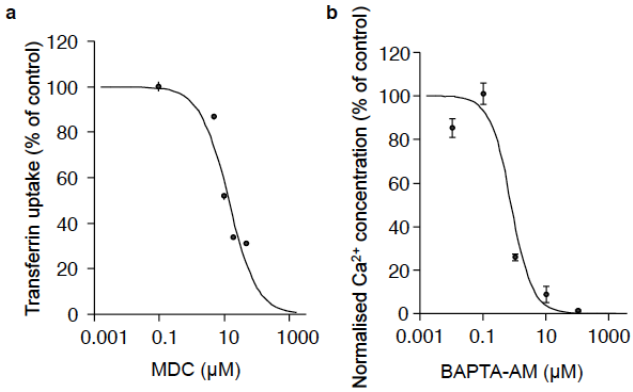
Supplementary Figure S11 | ROCK mediates RhoA signalling during IAV infection in a manner independent of its kinase activity. (**a**) MEFs were transfected for 48 h with siRNAs (#1 or #2) specific for ROCK1 or ROCK2 mRNAs or with a scrambled siRNA as a control, after which the amounts of ROCK1 and ROCK2 mRNAs were determined by reverse transcription and quantitative polymerase chain reaction analysis. "Mixture" indicates that cells were transfected with all four ROCK siRNAs. Error bars indicated s.d.. **P* < 0.05, ***P* < 0.01 versus control (scramble RNAi) (Student's *t*-test, data are from three independent experiments [*n* = 3 each]) (**b**) MEFs transfected as in (**a**) were subjected to immunoblot analysis with antibodies to ROCK1, ROCK2 or β-actin (loading control). The relative expression levels of ROCK1 and ROCK2, normalised by that of β-actin, were determined by densitometry and are indicated below each lane. S, scrambled siRNA; Mix, "Mixture" of all four ROCK siRNAs. (**c**) MEFs transfected for 48 h with scrambled or the mixture of ROCK siRNAs as in (**a**) were further transfected with an expression vector for YC3.60 for 24 h and subjected to Ca^{2+} imaging with exposure to PR8 at time 0. Data are representative of Ca^{2+} oscillations observed in a total of 10 cells.



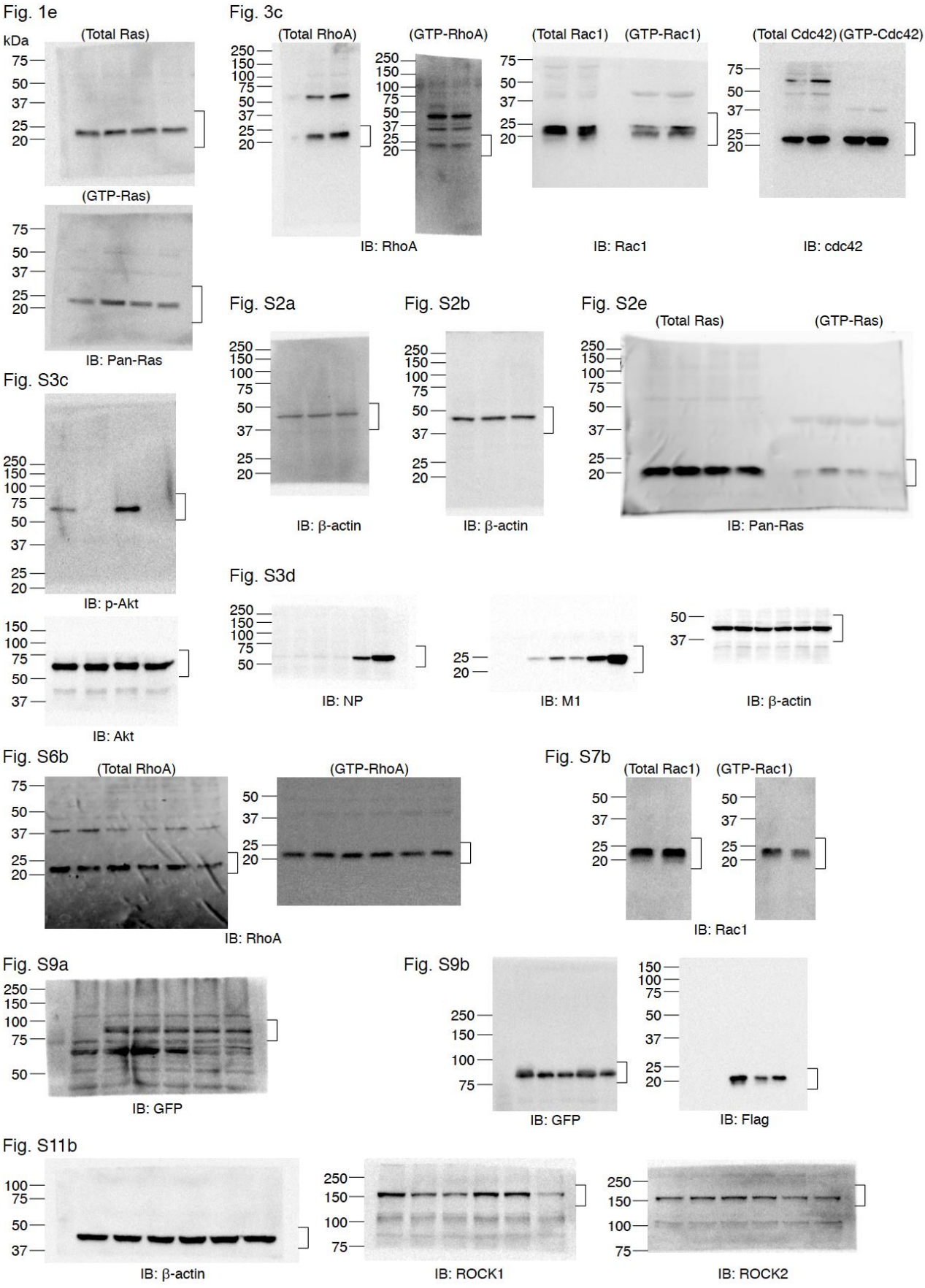
Supplementary Figure S12 | PLC participates in the induction of Ca^{2+} oscillations by RhoA. (**a**) Cos-1 cells expressing YC3.60 were incubated in the absence (red) or presence of 10 µM edelfosine (blue) for 30 min before infection with PR8 at time 0. The cells were monitored for Ca^{2+} transitions. (**b**) Cos-1 cells expressing GFP-Rab7 were incubated in the absence or presence of 10 µM edelfosine for 30 min and were then infected with PR8 for 1 h. Virus internalisation was evaluated. The boundaries of the box, the whiskers above and below the box and the line within the box represent the 25th and 75th percentiles, the 5th and 95th percentiles and the median value, respectively. $^{**}P < 0.01$ versus control cells (Student's *t*-test, $n = 15$) (**c**) Cos-1 cells expressing Raichu-RhoA were subjected to time-lapse microscopy with retreatment of edelfosine or U73122 for 30 min before exposure to PR8 at time 0. Error bars indicate s.e.m ($n = 5$).



Supplementary Figure S13 | IAV infection promotes clathrin-dependent and -independent endocytosis. MDCK cells were incubated with fluorescent transferrin (**a**) or dextran (**b**) for 10 min in the presence or absence of PR8 at an MOI of 10 (low) or 30 (high). The cells were then subjected to evaluation of endocytosis, as described. The boundaries of the box, the whiskers above and below the box and the line within the box represent the 25th and 75th percentiles, the 5th and 95th percentiles and the median value, respectively. *$P < 0.05$, **$P < 0.01$ versus Mock (Student *t*-test, $n = 20$).



Supplementary Figure S14 | Dose-response relationships of MDC and BAPTA-AM. (**a**) MDCK cells were incubated in the absence or presence of MDC at indicated concentrations for 30 min before exposure to fluorescently labelled transferrin for 10 min. The uptake of transferrin was then determined by measurement of fluorescence intensity. (**b**) MDCK cells expressing YC3.60 were incubated in the absence or presence of BAPTA-AM at indicated concentrations for 30 min and observed by fluorescence microscopy to monitor $[Ca^{2+}]_i$. Error bards indicate s.d. ($n = 3$ each)



Supplementary Figure S15 | Full scans of immunoblots. "]" indicates region displayed in the main figures.